Cement & Concrete Composites 33 (2011) 497–505

Contents lists available at ScienceDirect

Cement & Concrete Composites

journal homepage: www.elsevier.com/locate/cemconcomp

Self-healing efficiency of cementitious materials containing tubular capsules filled with healing agent

Kim Van Tittelboom [a], Nele De Belie [a,*], Denis Van Loo [b], Patric Jacobs [c]

[a] Magnel Laboratory for Concrete Research, Department of Structural Engineering, Faculty of Engineering, Ghent University, Technologiepark Zwijnaarde 904, B-9052 Ghent, Belgium
[b] Centre for X-ray Tomography, Department of Physics and Astronomy, Faculty of Sciences, Ghent University, Proeftuinstraat 86, B-9000 Ghent, Belgium
[c] Centre for X-ray Tomography, Department of Geology and Soil Science, Faculty of Sciences, Ghent University, Krijgslaan 281 S8, B-9000 Ghent, Belgium

ARTICLE INFO

Article history:
Received 19 April 2010
Received in revised form 26 November 2010
Accepted 9 January 2011
Available online 18 January 2011

Keywords:
Mortar
Cracks
Autonomous healing
Polyurethane
X-ray Computed Tomography

ABSTRACT

It has been estimated that, in Europe, 50% of the annual construction budget is spent on rehabilitation and repair of the existing structures [1]. Therefore, autonomous crack healing of concrete, a construction material that is highly susceptible to cracking, would be desirable. In this research, an encapsulated healing agent was embedded in the mortar matrix to obtain self-healing properties. Upon crack appearance, the capsules break and the healing agent is released, causing crack repair. By means of Computed Tomography and visual observation of the crack faces, filling of the cracks with healing agent was observed. It was seen that more than 50% of the original strength and stiffness could be regained after self-healing. It was also found that the water permeability could be reduced by a factor 10^2 to 10^4 due to autonomous crack healing. As a consequence, the proposed technique may be used for partial restoration of concrete properties after cracking.

1. Introduction

Striving for larger and more complicated structures, a variety of engineered materials with high-grade properties have become available. As stated by Van der Zwaag [2], however, these materials are almost always designed along the 'damage prevention principle'. This means that strength and stiffness properties of these materials are optimized in order to prevent the occurrence of damage. But during use, formation of damage can never be excluded completely. Consequently, structures made according to this principle will need periodic inspection to monitor damage and possibly costly repairs if damage is observed.

In the case of concrete, the occurrence of cracks is inevitable. Concrete can bear high compressive stresses, however, its tensile strength is limited. In the tension zone, concrete will always exhibit cracks. In the initial stage, this causes no problems relating to the load bearing capacity but it does potentially generate durability problems. Aggressive liquids and gasses may enter these cracks and they may cause concrete degradation. Because of such cracking, aggressive substances may reach the steel reinforcement and induce corrosion that may lead to further concrete damage and possibly structural failure.

From these findings, it may be concluded that, especially in the case of concrete, it would be more interesting to design according to the 'damage management concept', introduced by Van der Zwaag [2] and inspired by biological materials. Similar to broken bones that are able to heal autonomously, and damaged skin which may self-regenerate, we need to re-design the materials in order that the formation of damage is counteracted by a subsequent autonomous process of healing the damage. This means that the empty spaces created by cracks and defects need to be filled by new matter in order to seal the cracks, so that aggressive substances may not longer enter, and eventually mechanical properties are restored.

To fill the empty spaces created by cracks, some material needs to be transferred to the location of the defect. Consequently, a mobile liquid healing agent is needed. The viscosity of the healing agent should be low, so it can reach the various-sized cracks within the damage zone, including microcracks. Once this agent reaches these cracks it should preferentially expand to fill crack volumes much larger than that occupied by this liquid agent before the occurrence of damage. Another requisite for the healing agent is that it must form a sufficiently strong bond between the crack faces. Furthermore, carriers are needed which contain the healing agent and which are able to sense damage and trigger the healing mechanism by releasing the healing agent. Brittle materials that are embedded inside the cementitious matrix and break whenever cracks in the matrix appear may be suitable. In addition, the encapsulation material should exhibit good adhesion to the matrix and limited extension in order to rupture upon concrete cracking.

Several types of healing agents have already been tested in research on self-healing of concrete. Mostly single-component,

* Corresponding author. Tel.: +32 9 264 55 22; fax: +32 9 264 58 45.
E-mail address: nele.debelie@UGent.be (N. De Belie).

0958-9465/$ - see front matter © 2011 Elsevier Ltd. All rights reserved.
doi:10.1016/j.cemconcomp.2011.01.004

air-curing healing agents, such as cyanoacrylates [3–5], epoxy [6,7], silicons [4] or alkali-silica solutions [8], are preferred above multi-component healing agents, because incomplete mixing of the different components is feared. However, Dry and McMillan [9] stated that the potentially short shelf life of single-component healing agents might be disadvantageous. They mentioned that multi-component healing agents have more stability than single-component healing agents because they are activated at a later date, i.e. in situ. Therefore, they proposed the use of a multi-component methylmethacrylate system [9,10] and two-component epoxy resins [4].

In most investigations hollow glass tubes are used as encapsulation material [3–5,7–11]. In that case, the release of healing agent is activated by crack formation, which results in breakage of the embedded brittle glass tubes. The internal diameter of the tubes used ranges from 0.8 mm [3] to 4 mm [7]. Although these diameters are quite large, Joseph et al. [5] found that after crack formation only a small amount of the healing agent was drawn into the crack and that most of it remained inside the tubes due to the capillary forces. Therefore, they decided that tubes with open ends would be better as this would eliminate the suction effects of the closed ends [5]. Also Mihashi et al. [8] and Dry [11] made use of this technique in which continuous hollow glass tubes were embedded inside the specimens and were connected with a reservoir at the outside. Another advantage of this technique is that an additional amount of healing agent may be supplied when needed, so that larger cracks or a greater amount of cracks may be healed. However, as the healing agent needs to be supplied into the reservoir, this technique cannot be fully considered as self-healing.

In the research presented here, a two-component polyurethane foam was used as healing agent. Both components of the healing agent have low viscosity and the polymerization reaction does not depend on the mix ratio of both compounds. In addition, this agent expands upon reaction, providing a double advantage. In the first place, the expanding reaction acts as a driving force, pushing the healing agent out of the tubular capsules upon crack formation. A second advantage of this expanding reaction is that the additional volume created by the crack may be filled up with this healing agent without leaving too many gaps behind. As the glass capsules, used in most studies, may have a negative effect on the concrete durability (alkali-silica-reaction), in addition to glass, an alternative encapsulation material i.e. ceramics was studied in this research. Moreover, the influence of the tube diameter on the release of healing agent was investigated. Inside the cementitious matrix, two tubes, each containing one of both components of the healing agent, were positioned adjacent to each other. When cracking occurs at a certain place, these tubes break and both components may easily come into contact and subsequently heal the crack.

As cracking and crack healing occur internally, High Resolution X-ray Computed Tomography (HRXCT) was used as a non-destructive test method to evaluate the crack healing efficiency. HRXCT has already been used in previous research on self-healing materials [12–14], however, contradictory judgments were formulated about the effectiveness of this technique. Tan et al. [13] were able to visualize breakage of the encapsulation material, however, as the resolution was limited, they were not able to detect micro cracking so there was no indication whether the healing agent had infiltrated the cracks. In contrast, good results were obtained in the study of Mookhoek et al. [14]. They were able to distinguish full and empty capsules in self-healing composites and they succeeded to visualize healing of the crack. Besides making use of HRXCT, the efficiency of the proposed self-healing technique was also evaluated by means of mechanical tests, water permeability tests and evaluation of the cross sections.

2. Materials and methods

2.1. Tubular capsules filled with healing agent

Tubular capsules were used to carry the healing agent and to trigger the healing action upon crack appearance. In this research, the efficiency of tubes made from glass and tubes made from ceramics was compared. In addition to high hardness and strength, glass and ceramics possess a high brittleness. Due to the latter, these tubes will easily break whenever cracks appear in the mortar matrix. Borosilicate glass tubes were purchased from the Hilgenberg company in Frankfurt. The ceramic tubes were manufactured by VITO (Flemish Institute for Technological Research). More information concerning the preparation of the ceramic tubes can be found in Buysse et al. [15]. In order to investigate the effect of the tube diameter, tubes with a different internal diameter but with the same internal volume were used. An overview of the tube dimensions is given in Table 1.

MEYCO MP 355 1K (BASF The Chemical Company) was used in this study as healing agent. MEYCO is a commercially available healing agent that is used in practice to make cracks watertight and to cut off running water. This product consists of two compounds with a viscosity of 600 mPa s and 70 mPa s at 23 °C, respectively. One compound consists of a prepolymer of polyurethane and starts foaming in moist surroundings. The second compound is an accelerator that shortens the reaction time. The expanding foaming reaction of this healing agent may lead to an increase in volume of 25–30 times. Because of this, the additional volume created by the cracks may be filled up again.

Half of the tubes was filled with the prepolymer and the other half was filled with a mixture of accelerator and water. First, the tubes were sealed with polymethylmethacrylate at one end, then, the tubes were filled with the components of the healing agent, which were injected by means of a syringe with a needle. When all tubes were filled, the other ends were sealed and the tubes were ready to be embedded inside the mortar samples. Inside the mortar specimens, both tubes, containing the prepolymer and the accelerator, were positioned next to each other.

2.2. Mortar samples with(out) self-healing properties

Mortar with a water to cement ratio of 0.5 and a sand to cement ratio of 3 was made by using ordinary Portland cement (CEM I 52.5 N). Specimens with two different geometries were used.

For the first experiment, prismatic moulds with dimensions of 60 mm × 60 mm × 220 mm, provided with a 5 mm deep notch at the lower side, were used (Fig. 1A). First, a 10 mm mortar layer was brought into the moulds. When this layer was compacted by means of vibration, two reinforcement bars (diameter 2 mm) and two couples of tubes (with one tube of each couple filled with the prepolymer and the other tube filled with a mix of accelerator and water) were placed on top of it. Afterwards, the moulds were completely filled with mortar and vibrated. The reference samples (REF) and samples used for manual crack healing (MAN) were prepared in the same way as described above, however, samples belonging to these series contained two reinforcement bars only (Table 2).

For a second experiment, cylindrical moulds with a diameter of 76 mm and a height of 20 mm were used (Fig. 1B). Again, a mortar layer of 10 mm was brought into the moulds and compacted by means of vibration. Two steel fibers (diameter 1 mm) and three couples of tubes were placed on top of this layer. Afterwards, the moulds were completely filled and vibrated. The test series 'UNCR, REF and MAN' only contained two steel fibers inside the matrix (Table 2).

Table 1
Dimensions of the tubes used for encapsulation of the healing agent.

Specimen	Name	Material	$\varnothing_i$ (mm)	$\varnothing_o$ (mm)	Length (mm)	Volume (mm^3)
Prism	GLA-2	Glass	2.00	2.20	82.60	259.24
	GLA-3	Glass	3.00	3.35	36.70	259.24
	CER	Ceramics	2.57	2.99	50.00	259.24
Cylinder	GLA-2	Glass	2.00	2.20	41.30	129.62
	GLA-3	Glass	3.00	3.35	18.40	129.62
	CER	Ceramics	3.34	3.86	15.00	129.62

After casting, all moulds were placed in an air-conditioned room with a temperature of 20 ± 2 °C and a relative humidity of 90 ± 10% for a period of 24 h. After demoulding, the specimens were stored under the same conditions for 6 subsequent days.

2.3. Creation of cracks

2.3.1. Three-point-bending test

At the age of 7 days, the mortar prisms were cracked, and thus for the prisms containing embedded healing agent the healing mechanism was triggered, by means of a crack width controlled three-point-bending test. The crack width was measured by means of a linear variable differential transformer (LVDT, Solartron AX/0.5/S) with a measurement range of ±500 μm and an accuracy of 1 μm. The LVDT was attached at the bottom of the mortar sample, as shown in Fig. 1A. The crack width was increased with a velocity of 0.5 μm/s until a crack of 400 μm was reached. At that point, the specimen was unloaded giving cause to a decrease in crack width. The resulting crack width amounted approximately 220 μm.

Table 2
Composition of the test specimens.

Specimen	Name	Crack	Crack treatment	Encapsulation material	Number of samples
Prism	REF	Yes	No treatment	–	3
	MAN	Yes	Manual healing	–	3
	GLA-2	Yes	Autonomous healing	Glass tubes	3
	GLA-3	Yes	Autonomous healing	Glass tubes	3
	CER	Yes	Autonomous healing	Ceramic tubes	3
Cylinder	UNCR	No	–	–	4
	REF	Yes	No treatment	–	4
	MAN	Yes	Manual healing	–	4
	GLA-2	Yes	Autonomous healing	Glass tubes	4
	GLA-3	Yes	Autonomous healing	Glass tubes	4
	CER	Yes	Autonomous healing	Ceramic tubes	4

2.3.2. Splitting test

In the cylindrical mortar specimens, cracks were created at 7 days age by means of a crack width controlled splitting test. In this case, the crack width was measured at both sides of the specimen and the mean value was used to control the splitting test. For this purpose, an LVDT was attached on each side of the specimen at middle height (Fig. 1B). Again, the crack width was increased with a velocity of 0.5 μm/s until a crack with a width of 400 μm was reached. Then, specimens were unloaded giving rise to a final crack width of approximately 250 μm.

2.4. Crack healing

Cracks of the specimens containing encapsulated healing agent were autonomously healed. The embedded tubes broke during

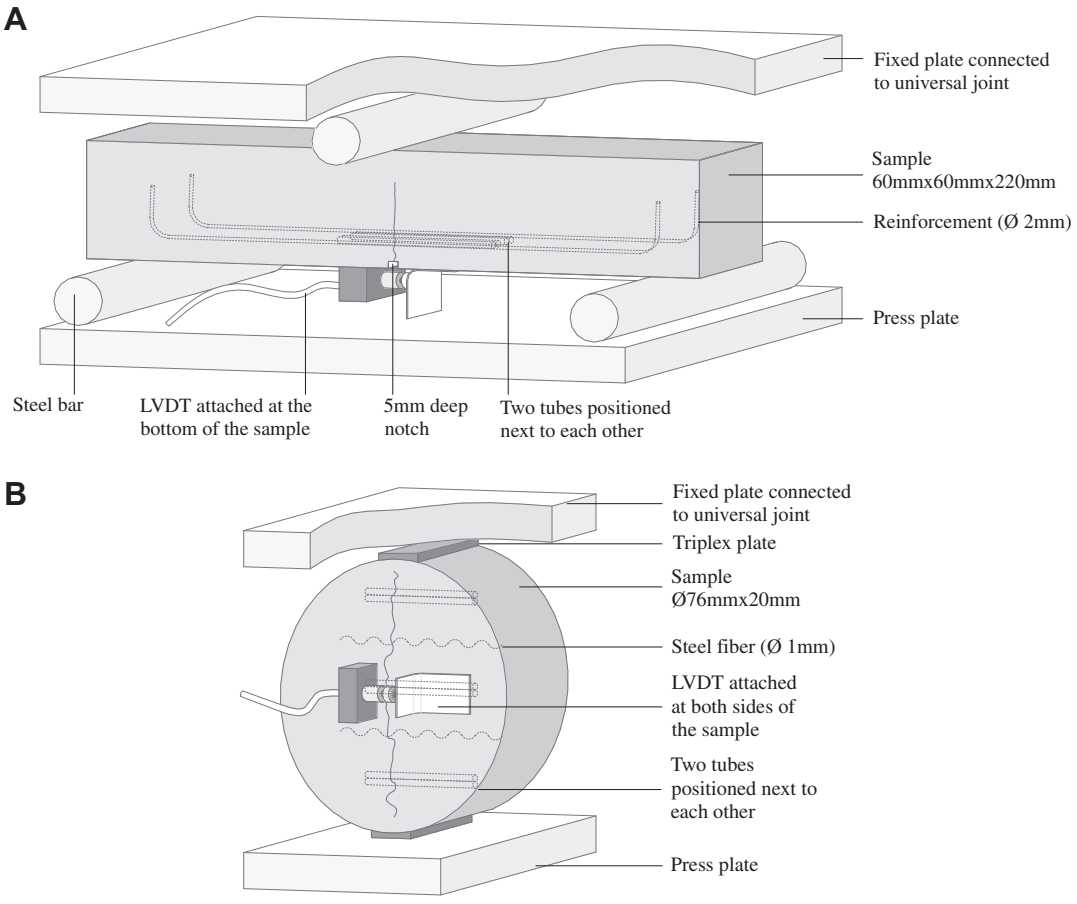

Fig. 1. Setup of the three-point bending test (A) and splitting test (B).

crack formation and both components of the healing agent were released into the crack due to capillary forces. Upon contact of both components, polyurethane foam was formed, resulting in crack healing. Cracks of the samples belonging to the test series 'MAN' were treated immediately after crack formation. First, the prepolymer was mixed with water and accelerator in the same proportions as encapsulated in the tubes. Next, the mixture was injected into the crack by means of a syringe with a needle. Injection was stopped when the crack was completely filled with the healing agent.

2.5. Evaluation of the healing efficiency

2.5.1. Regain in mechanical properties

One day after crack creation, when the polyurethane inside the cracks of the manually healed and autonomously healed specimens was thought to have hardened (reaction time of the polyurethane takes only a few minutes), all prisms were reloaded in three-point-bending to evaluate the healing efficiency. The first prism tested was completely broken after this reloading cycle. As it was observed that the crack faces were wet, indicating that some additional healing agent came out of the tubes upon reloading, the remaining prisms were also subjected to a second reloading cycle 1 day later. However, cracks of the test series 'MAN' were not injected again with healing agent in between the first and the second reloading cycle.

From the obtained loading curves, the strength and the stiffness of the beams was calculated and the mechanical properties after (self-)healing were compared with the original values. The peak load F_c, was used as an indication for the strength while the slope of the curve, joining the points $0F_c$ and $0.4F_c$ was used to indicate the stiffness. The method used to determine the stiffness is based on the method to calculate the *E*-modulus according to the standard NBN B 15-002 [16].

2.5.2. Decrease in water permeability

The cracked and uncracked specimens were subjected to a water permeability test in order to investigate the efficiency of the (self-)healing mechanism. A complete description of the test procedure, based on the method provided by Aldea et al. [17], is given in Van Tittelboom et al. [18]. Briefly, samples were vacuum saturated and subsequently mounted in the test setup shown in Fig. 2. The drop in water level, due to water flow through the specimen, was measured at regular time intervals and water was added each time to the original level. Darcy's law (Eq. (1)) was used to calculate the coefficient of water permeability *k*.

$$k = \frac{aT}{At} \ln\left(\frac{h_0}{h_f}\right) \tag{1}$$

where *a* is the cross sectional area of the pipette, measured in square metres; *A* is the cross sectional area of the specimen, measured in square metres; *T* is the specimen thickness, in metres; *t* is the time, in seconds; h_0 and h_f are the initial and final water heads, measured in centimetres.

The water permeability measured was not immediately constant but decreased during several days. Consequently, measurements were repeated until a steady state flow was reached. A steady state flow was considered to have been reached when similar results, for the drop in water level, were obtained during 5 subsequent days. The calculated coefficient of water permeability was based on the average of the latest five measurements.

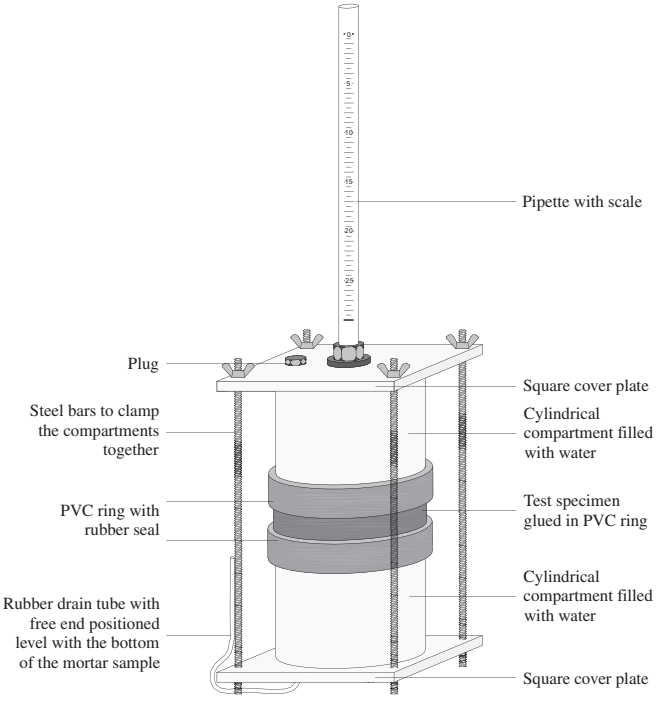

Fig. 2. Setup of the water permeability test.

2.5.3. Visualization of the crack region by means of High Resolution X-ray Computed Tomography

After samples were tested for regain in mechanical properties, they were scanned using the in-house developed HRXCT system of the Centre for X-ray Tomography of Ghent University (UGCT) [19]. The system is composed of an X-ray tube, a flat panel detector and a rotation stage. For each of the samples 1200 projections were taken at 0.3° of rotation interval over 360°. The mortar samples were scanned at 150 kV tube voltage and with a 2 mm Cu filter. The projection data were reconstructed into HRXCT slices using Octopus [20]. In order to analyse and visualize the data, the reconstructed datasets for each sample were loaded in the analysis software Morpho+ [20] where a selection was made of the crack region and subsequently of the tubular capsules. These selected datasets were loaded into VGStudio [21] and based on the grey values, the polyurethane foam inside the crack and the tubes was selected and visualized by means of a yellow colour. Finally the treated datasets were combined with the original dataset of the mortar matrix.

2.5.4. Evaluation of the cross sections

After performing the HRXCT-scans, prismatic specimens were completely broken and photographs were taken from the cross sections. The percentage of the surface covered with polyurethane was calculated by means of the software ImageJ [22]. Based on the size of the area covered with healing agent, a comparison was made between the effectiveness of self-healing of mortar specimens containing tubes with different tube diameters and made of different encapsulation materials.

2.6. Statistical analysis of the data

For each of the experiments, an analysis of variance test (ANOVA-test) was applied to determine whether or not the means of various groups were equal. First, homogeneity of the variances was verified by means of a Levene's test (significance level 0.01). When equal variances were assumed, a Student–Newman–Keuls test (significance level 0.05) was performed. For data with non-homogeneous variances, a Dunnett's T3 test (significance level 0.05) was used.

3. Results and discussion

3.1. Effect of the encapsulation material on the strength

Although the concrete layer is not of much structural importance in the tension zone, the strength of the concrete layer may not be reduced too much, because the lower the concrete tensile strength, the sooner cracks appear. Therefore, the effect of the tubular capsules on the tensile strength of the mortar specimens was investigated. During the bending test and the splitting test, the original tensile strengths of plain mortar specimens (REF and MAN) were compared with the tensile strengths of specimens containing tubes (GLA_2, GLA_3 and CER). The results obtained from the tensile splitting test, presented in Fig. 3, showed no significant difference in strength between the different test series. Concerning the mean flexural strength (Fig. 3), it was even seen that a higher strength was obtained when ceramic tubes were incorporated. From these results, it may be concluded that incorporation of encapsulation materials does not result in a significantly different tensile strength.

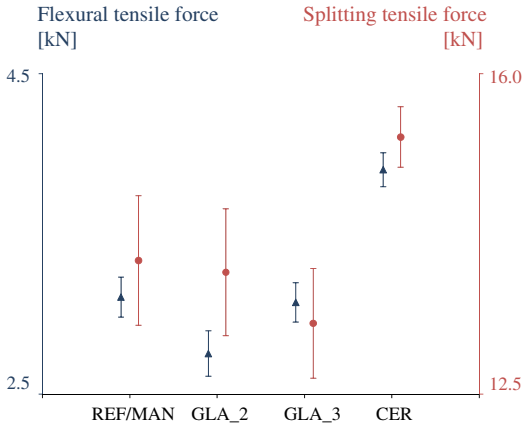

Fig. 3. Comparison of the initial flexural tensile force (▲, $n = 3$) and splitting tensile force (●, $n = 4$) for the different test series. Symbols represent the mean value while error bars are used to indicate the standard error.

3.2. Regain in mechanical properties

During crack formation, it was seen that the load first increased without much displacement (Fig. 4). As reaching of the peak load was accompanied with appearance of the crack, from this moment on, the load decreased and the crack width was increasing continuously. When a crack width of ±100 μm was reached, the load started to increase again. This increase in load was caused by the reinforcement inside the mortar specimens. When a crack width of 400 μm was reached, the specimens were unloaded and it can be observed in Fig. 4 that at this moment the crack width decreased because of the elastic properties of the mortar and steel. For the untreated specimens and the specimens for which cracks were manually healed, the curves obtained during crack formation

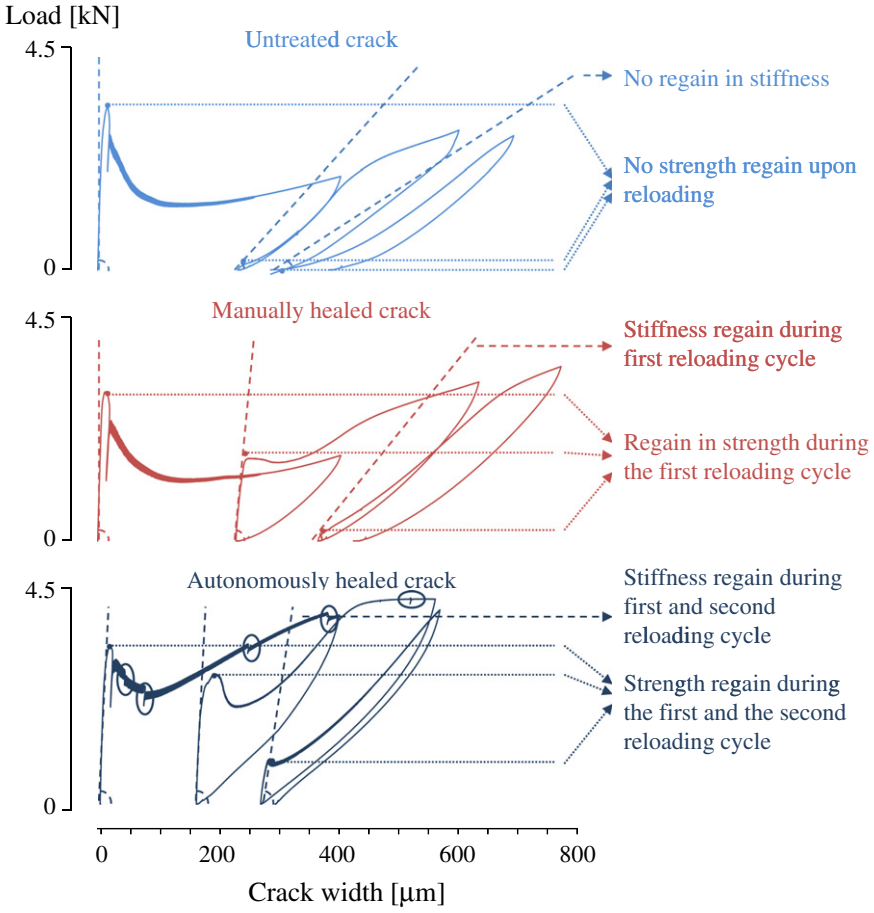

Fig. 4. Loading curves obtained during crack formation and during the first and the second reloading cycle for untreated cracks (REF), manually healed cracks (MAN) and autonomously healed cracks (GLA_3). The obtained peak loads were used as an indication of the strength while the slope of the first part of the curve was utilized to indicate the stiffness. Drops in load due to breakage of the tubular capsules are indicated by means of an ellipse.

looked similar. In the graph representing the result of a specimen with self-healing properties, some distinct drops in load were observed after the peak load had been reached. These drops in load were related to breakage of the tubular capsules as these drops were accompanied with audible 'pop' sounds. These findings are consistent with those of Thao et al. [7].

During the first reloading cycle, it was found that in the case of untreated cracks, the first part of the curve followed the last part of the previous curve. This indicated that no regain in mechanical properties was obtained. The crack just reopened upon reloading. However, when the curve, obtained during the first reloading cycle, of the manually healed and autonomously healed specimens was examined, a new peak load was observed. This indicated that regain in strength was obtained due to crack healing. Additionally, it was also observed that the first part of these curves had a steeper slope compared with the last part of the previous curves. This indicated that there was also regain in stiffness.

For the specimens with self-healing properties, again a small peak was observed during the second reloading cycle. This time, the peak load was much smaller compared with the peak during the first reloading cycle. From this, it may be concluded that the second autonomous healing action is less effective than the first one. Some additional healing agent was released upon reloading but this only led to little regain in mechanical properties. However, when cracks were manually healed, no new peak was observed during the second reloading cycle and so in this case, no mechanical properties were restored.

In Fig. 5A the amount of strength regain, obtained during the first and the second reloading cycle, is shown for all test series. It was observed that during the first reloading cycle only minimal strength was retrieved for the reference samples (REF), while for the repaired cracks, a higher regain in strength was noticed. In the case cracks were manually healed (MAN), an average strength regain of 61% was obtained. If encapsulated healing agents were present inside the mortar matrix, an average regain in strength of 54%, 62% and 48% was achieved for glass tubes with a diameter of 2 mm (GLA_2) and 3 mm (GLA_3) and for ceramic tubes (CER), respectively. Compared to the results obtained for the manually healed cracks, no significant difference in strength regain was noticed, during the first reloading cycle, when the cracks were healed autonomously. Moreover, specimens with encapsulated healing agents gave evidence of a second healing action. While reference samples and samples with manually healed cracks showed almost no retrieval in strength during the second reloading cycle, specimens with ceramic tubes inside showed a strength regain with an average value of 17%. Samples containing glass tubes with a diameter of 2 mm and 3 mm showed an average regain of 23% and 20%, respectively.

In Fig. 5B the amount of regain in stiffness is shown. During the first reloading cycle a significant difference in stiffness regain was observed between the reference samples (REF) and the manually (MAN) or autonomously healed samples (GLA_2, GLA_3 and CER). While almost no regain in stiffness was obtained for reference samples, an average stiffness regain between 40% and 64% was obtained when cracks were repaired with polyurethane. Again, based on the amount of regain in stiffness, no significant difference was seen between the efficiency of manual and autonomous crack healing. During the second reloading cycle stiffness regain decreased till an average value of 7% for the manually healed samples while the specimens with embedded tubes gave evidence of a second healing action and thus a higher stiffness recovery. Specimens with embedded glass tubes, with a diameter of 2 mm and 3 mm and specimens with embedded ceramic tubes showed a second stiffness recovery of 34%, 21% and 32%, respectively.

The advantage of encapsulation of the healing agent is that multiple healing cycles may be obtained while the healing efficiency during the first cycle is comparable with the efficiency of manual crack healing. However, from the margin of error shown in the graph, it may be concluded that the self-healing action is more liable to coincidental effects, e.g. breakage of the tubes, amount of healing agent coming out of the tubes. Based on these results there is no significant difference between the efficiency of glass tubes and ceramic tubes, nor between glass tubes with an internal diameter of 2 mm and 3 mm. Normally, the efficiency of emptying of the tubes is dependent on the capillary forces inside the tubes, which are reduced when the tube diameter increases. However, an alteration in the diameter of the glass tubes from 2 mm to 3 mm did not seem to give significant differences in outcome.

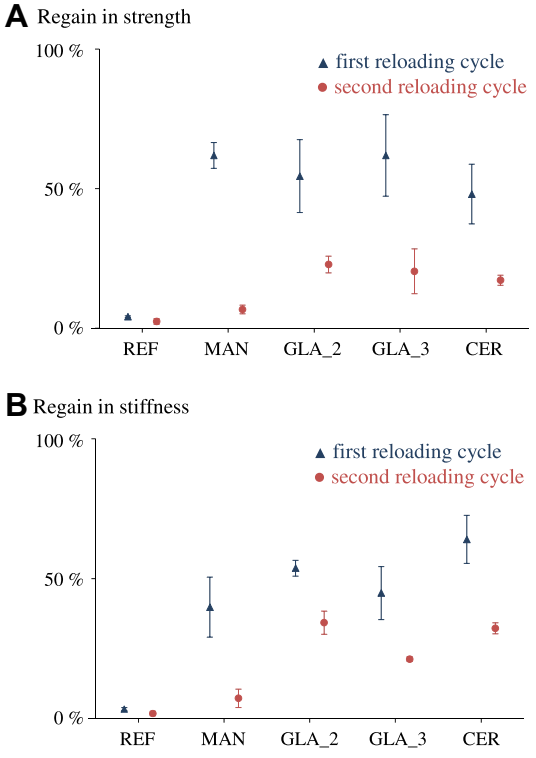

Fig. 5. Regain in strength (A) and stiffness (B) obtained during the first and the second reloading cycle. Symbols represent the mean values while error bars are used to indicate the standard error ($n = 3$).

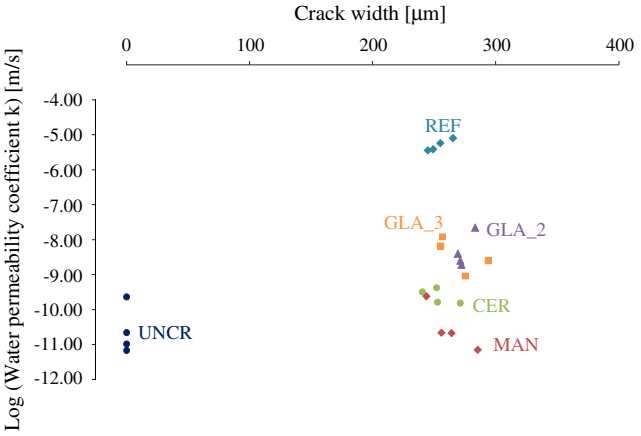

Fig. 6. Water permeability coefficient obtained for the different test series.

3.3. Decrease in water permeability

In Fig. 6, the water permeability coefficient is plotted against the crack width. To improve the clarity of the graph, log values of the water permeability coefficient are shown. The crack width shown in the graph is the average of the final crack width measured by both LVDTs used in the splitting test. When cracks were created in the specimens and these cracks were left untreated (REF), it was observed that the water permeability coefficient was 10^4 to 10^6 times higher compared to uncracked specimens (UNCR). When these cracks were treated manually (MAN) by means of polyurethane foam, a reduction of 10^4 to 10^5 was noticed. No significant difference was seen when comparing the water permeability coefficient obtained for specimens with manually healed cracks with the coefficient obtained for uncracked specimens, indicating that the polyurethane foam, used to seal the cracks, is very effective. Sealing of the cracks with this type of healing agent makes the cracked specimens as impermeable as uncracked specimens. If self-healing properties were built-in, the measured water permeability coefficient was slightly higher compared with manually healed cracks, however, it was possible to reduce the water permeability coefficient with a factor of 10^2 to 10^3 when glass tubes were used and even with a factor 10^3 to 10^4 when ceramic tubes were embedded. In this experiment, it was seen that encapsulation of the healing agent with ceramic tubes seemed to result in a significant better performance.

3.4. Visualization of the crack region by means of High Resolution X-ray Computed Tomography

Fig. 7 illustrates the 3D rendered dataset, showing the part of a mortar prism which contained the broken tubes and the crack. From this figure, it may be concluded that it is possible to visualize polyurethane foam inside a dense mortar matrix. Although the polyurethane foam had very low X-ray absorption compared to mortar, the remaining polyurethane inside the tubes and filling of the crack with polyurethane were clearly visible. The dark parts that were seen inside the tubes correspond to air bubbles which arose as part of the healing agent leaked out of the tubes into the crack after tube breakage. Furthermore, it was observed that the released healing agent was spread into the crack, which led to sealing of the crack faces. In order to compare the effectiveness of the three different encapsulation techniques under investigation, the scans, which resulted in slices in *Z*-direction were resliced in the *Y*-direction in order to get a cross section in the same plane as the four tubes. From Fig. 8 it became obvious that neither of the tubes had completely been emptied during crack formation. Although it was not really expected, it was seen that in the case of glass tubes with a diameter of 2 mm (Fig. 8A) the volume of healing agent released was comparable with the volume released for 3 mm diameter tubes (Fig. 8B). When comparing these results with the ones obtained when using ceramic tubes (Fig. 8C), some difference was observed. In Fig. 8C only 3 out of the 4 tubes were visible because the fourth tube was positioned somewhat lower than the other tubes. However, it was noticed that the ceramic tubes seemed to release more healing agent compared to the glass tubes. This may be caused by the difference in surface tension between glass and ceramics. Further research will be performed to find out the positive effect of using ceramic materials instead of glass. In addition to the content of the tubes, also filling of the crack was visualized using HRXCT. It was clearly visible where the

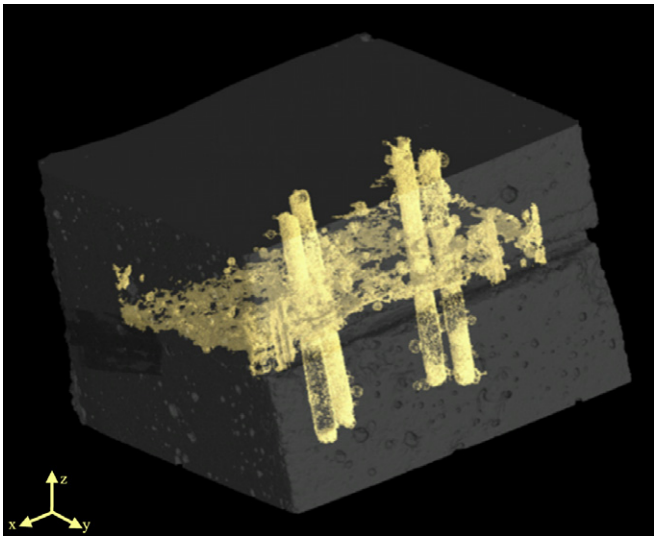

Fig. 7. 3D visualization of the region of the mortar sample which contained the tubes and the crack.

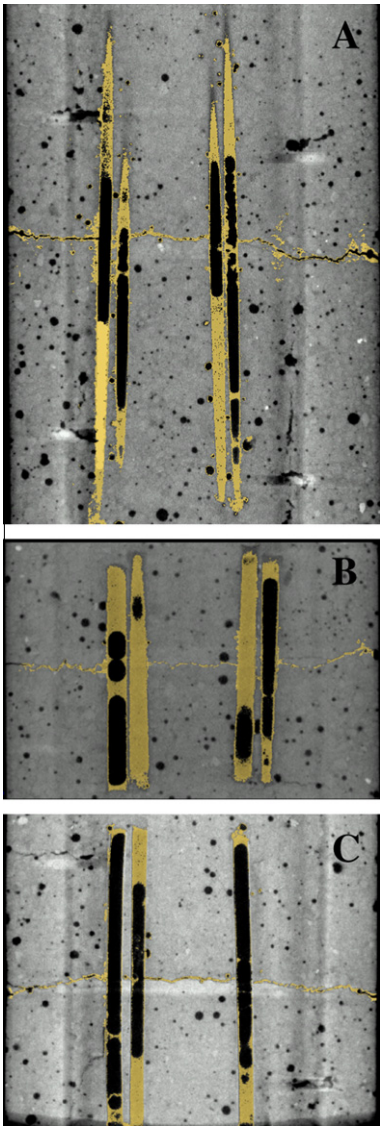

Fig. 8. *Y*-direction CT cross section through the glass tubes, (A) sample with 2 mm diameter glass tubes, (B) sample with 3 mm diameter glass tubes and (C) sample with ceramic tubes.

polyurethane foam had filled up the crack compared to regions where there was no polyurethane (Fig. 8).

Based on these results it may be concluded that HRXCT can be used to evaluate the efficiency of autonomous crack healing actions. Although it seemed possible to perform a qualitative evaluation of the healing efficiency, a quantitative evaluation, like it was done in the study of Mookhoek et al. [14] is not yet feasible. This may be explained by the fact that the experiments of Mookhoek et al. [14] were performed by means of a synchrotron light source, while we made use of a normal X-ray source. Whereas the quality of the scans obtained in this research is definitely lower, the used equipment is more easily available. In addition, we scanned real size mortar samples (60 mm × 60 mm × 220 mm) instead of the meticulous samples of some millimeters that have been used in the previous mentioned study. Based on the promising first results, further development of the HRXCT system could make it possible to perform a more comprehensive evaluation of the healing efficiency for concrete by visualizing breakage of the tubes and the release kinetics of the healing agent.

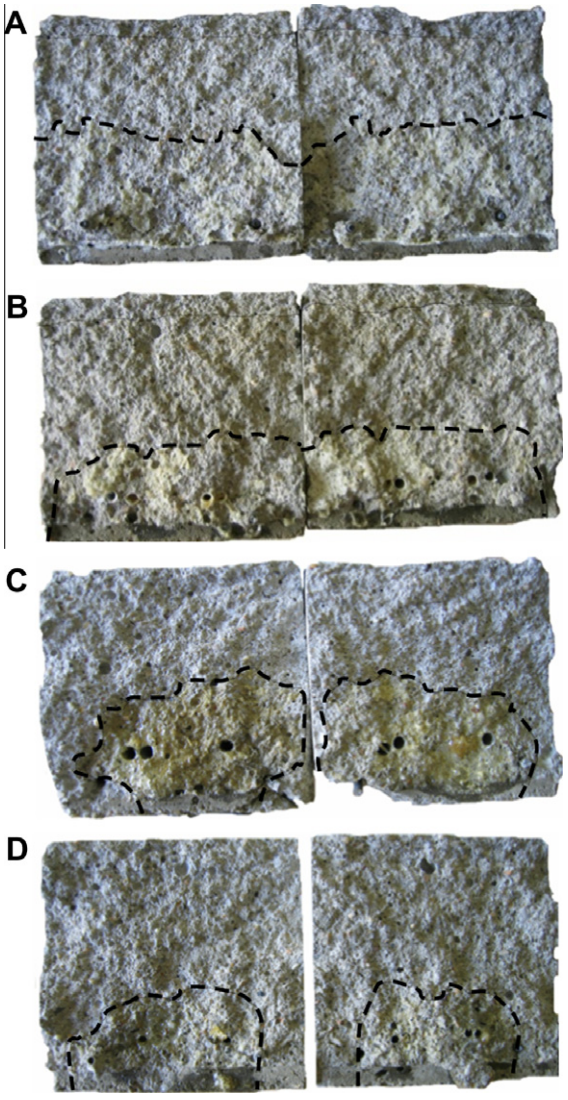

Fig. 9. Cross sections of mortar prisms containing two reinforcement bars and two double tubes filled with healing agent. The polyurethane migration front is indicated with a dashed line. The average covering with polyurethane amounted to 45% for manually healed cracks (A) and 36% in the case ceramic tubes (B) or glass tubes with a diameter of 3 mm (C) were used. For tubes with a diameter of 2 mm the average covering amounted to 24% (D).

3.5. Evaluation of the cross sections

For all test series, except the reference series, it was seen that the crack faces were partly covered with polyurethane foam. In the case cracks were manually healed, the healing agent was injected along the whole crack length. Consequently, it was seen that the healing agent was equally spread over the crack faces, covering almost half of the cross section (Fig. 9A). When cracks were autonomously healed, the healing agent was released from certain positions. However, due to the capillary forces inside the crack, the released healing agent moved further and was even able to move against gravitation. In the case ceramic tubes or glass tubes with a diameter of 3 mm were used, there was no significant difference in percentage of covering compared to manually healed cracks. While the average surface covering amounted 45% for manually healed cracks, 36% of covering was obtained for the 3 mm diameter glass tubes and for the ceramic tubes (see Fig. 9B and C). As it may be seen in Fig. 9D, a significant different amount of covering was noticed when 2 mm diameter glass tubes were used as encapsulation material. In the latter case, an average covering of only 24% was reached and the healing agent was more localized around the tubes. This may be because the capillary forces, which tried to keep the healing agent inside the tubes, were bigger when the tube diameter was smaller. However, this difference in efficiency was not observed from the other experiments.

4. Conclusions and future perspectives

From these results it can be concluded that the polyurethane used in this research is a very appropriate healing agent for obtaining self-healing properties in cementitious materials. The key factor of this healing agent is its ability to expand. This enables healing of larger crack openings, which is a big advantage in the development of self-healing concrete.

In most of the experiments the glass and ceramic tubes showed similar performance, however from the water permeability tests and the HRXCT-scans it was observed that better results were obtained when ceramic tubes were used. The difference in efficiency between glass and ceramics as encapsulation material will be the subject of further research.

Both encapsulation materials used are brittle so they easily break and release the healing agent when cracks appear. However, upon casting of the specimens care should be taken to prevent early rupture of the tubes. Moreover, in these experiments, the tubes were positioned at the exact location of crack formation while in reality the location of crack formation will not be known. It is the intention of the authors to randomly distribute capsule pairs throughout the regions susceptible to cracking. As a consequence, the capsules need to be mixed in and survive the mixing process. Therefore, the integrity of the capsules during mixing will be investigated in the future. At that time, concrete will be used instead of mortar because rubbing of the aggregates will have an additional negative effect on the capsules during mixing.

It was seen that the water permeability coefficient obtained for manually healed cracks was equal to the coefficient obtained for uncracked specimens. In the case cracks were autonomously healed, the obtained water permeability coefficients were slightly higher but compared to untreated cracks, a reduction with a factor of 10^2 to 10^4 was seen. If the water, penetrating into the cracks, would contain aggressive substances, it is clear that sealing of the cracks by self-healing activity (even if not 100% efficient), would greatly reduce the degradation rate and increase the service life of the structure.

It may also be concluded that autonomous crack healing results in retrieval of mechanical properties with an equal efficiency as

manual crack healing. Self-healing of cracks has the added advantage that a second healing action may occur. As the used polyurethane is a porous foam, the percentage of retrieval in mechanical properties was limited. However, the most important objective of autonomous crack repair is that the cracks become sealed, reducing the potential for reinforcing steel corrosion.

HRXCT has been used for the first time to evaluate the self-healing efficiency in cementitious materials. Based on the promising first results it may be concluded that this technique is useful to study breakage of the capsules and crack filling.

The authors believe that the proposed self-healing mechanism will be useful to implement into concrete structures that are not easily accessible for maintenance and repair such as underground structures, bridges, and dams. Although, the initial costs will be higher, maintenance costs can be reduced and the service life of the structures may be extended as damage is immediately repaired.

Acknowledgements

Financial support from the Research Foundation Flanders (FWO-Vlaanderen) for this study (Project No. G.0157.08) is gratefully acknowledged. The authors would like to thank Jianyun Wang and Willem De Muynck for critically reading the manuscript.

References

[1] Cailleux E, Pollet V. Investigations on the development of self-healing properties in protective coatings for concrete and repair mortars. In: Proceedings of the second international conference on self-healing materials; 2009. p. 120.
[2] Van der Zwaag S. An introduction to material design principles: damage prevention versus damage management. In: van der Zwaag S, editor. Self healing materials. An alternative approach to 20 centuries of materials science. Springer Netherlands: Springer series in materials science; 2007. p. 1–18.
[3] Li VC, Lim YM, Chan Y-W. Feasibility study of a passive smart self-healing cementitious composite. Compos Part B: Eng 1998;29(6):819–27.
[4] Dry C. Design of self-growing, self-sensing and self-repairing materials for engineering applications. In: Wilson AR, Asanuma H, editors. Proceedings of the society of photo-optical instrumentation engineers (SPIE); 2001. p. 23–29.
[5] Joseph C, Jefferson AD, Canoni MB. Issues relating to the autonomic healing of cementitious materials. In: Proceedings of the first international conference on self-healing materials; 2007. p. 1–8.
[6] Nishiwaki T, Mihashi H, Jang B-K, Miura K. Development of self-healing system for concrete with selective heating around crack. J Adv Concr Technol 2006;4(2):267–75.
[7] Thao TDP, Johnson TJS, Tong QS, Dai PS. Implementation of self-healing concrete - Proof of concept. IES J Part A: Civ Struct Eng 2009;2(2):116–25.
[8] Mihashi H, Kaneko Y, Nishiwaki T, Otsuka K. Fundamental study on development of intelligent concrete characterized by self-healing capability for strength. Trans Jpn Concr Inst 2000;22:441–50.
[9] Dry C, McMillan W. Three-part methylmethacrylate adhesive system as an internal delivery system for smart responsive concrete. Smart Mater Struct 1996;5:297–300.
[10] Dry C. Matrix cracking repair and filling using active and passive modes for smart timed release of chemicals from fibers into cement matrices. Smart Mater Struct 1994;3:118–23.
[11] Dry C, Corsaw M. A comparison of bending strength between adhesive and steel reinforced concrete with steel only reinforced concrete. Cem Concr Res 2003;33(11):1723–7.
[12] Garcia A, Schlangen E, van de Ven M, Liu Q. Electrical conductivity of asphalt mortar containing conductive fibers and fillers. Construct Build Mater 2009;23(10):3175–81.
[13] Tan PS, Zhang MQ, Bhattacharyya D. Processing and performance of self-healing materials. In: IOP conference series: materials science and engineering; 2009.
[14] Mookhoek SD, Mayo SC, Hughes AE, Furman SA, Fischer HR, van der Zwaag S, Ludwig W. Using synchrotron X-ray micro tomography to quantitatively analyze fracture and healing processes in self-healing thermoplastics. In: Proceedings of the second international conference on self-healing materials; 2009.
[15] Buysse C, Kovalevsky A, Snijkers F, Buekenhoudt A, Mullens S, Luyten J, et al. Fabrication and oxygen permeability of gastight, macrovoid-free $Ba_{0.5}Sr_{0.5}Co_{0.8}Fe_{0.2}O_{3-\delta}$ capillaries for high temperature gas separation. J Membr Sci 2010;359(1-2):86–92.
[16] NBN B 15-002: 1995. Eurocode 2: Berekeningen van constructies – Deel 1-1: Algemene regels en regels voor gebouwen.
[17] Aldea CM, Shah SP, Karr A. Permeability of cracked concrete. Mater Struct 1999;32(219):370–6.
[18] Van Tittelboom K, De Belie N, De Muynck W, Verstraete W. Use of bacteria to repair cracks in concrete. Cem Concr Res 2010;40(1):157–66.
[19] Masschaele BC, Cnudde V, Dierick M, Jacobs P, Van Hoorebeke L, Vlassenbroeck J. UGCT: new X-ray radiography and tomography facility. Nucl Instrum Method Phys Res – Sec A 2007;580(1):266–9.
[20] Vlassenbroeck J, Dierick M, Masschaele B, Cnudde V, Van Hoorebeke L, Jacobs P. Software tools for quantification of X-ray microtomography at the UGCT. Nucl Instrum Method Phys Res – Sec A 2007;580(1):442–5.
[21] VGStudio. <http://www.volumegraphics.com/>.
[22] Rasband WS. ImageJ. Bethesda, Maryland (USA, US): National Institutes of Health; 1997–2008. <http://rsb.info.nih.gov/ij/ed>.